

Direct observation of stepwise movement of a synthetic molecular transporter

Shelley F. J. Wickham¹, Masayuki Endo^{2,3}, Yousuke Katsuda⁴, Kumi Hidaka⁴, Jonathan Bath¹, Hiroshi Sugiyama^{2,3,4*} and Andrew J. Turberfield^{1*}

Controlled motion at the nanoscale can be achieved by using Watson-Crick base-pairing to direct the assembly and operation of a molecular transport system consisting of a track, a motor^{1–12} and fuel^{13–15}, all made from DNA. Here, we assemble a 100-nm-long DNA track on a two-dimensional scaffold¹⁶, and show that a DNA motor loaded at one end of the track moves autonomously and at a constant average speed along the full length of the track, a journey comprising 16 consecutive steps for the motor. Real-time atomic force microscopy allows direct observation of individual steps of a single motor, revealing mechanistic details of its operation. This precisely controlled, long-range transport could lead to the development of systems that could be programmed and routed by instructions encoded in the nucleotide sequences of the track and motor. Such systems might be used to create molecular assembly lines modelled on the ribosome.

An effective linear molecular motor must traverse its track without dissociating^{1–7,10,12} and run unidirectionally without external intervention^{4–12}. Directionality may be imposed by the sequential addition of DNA instructions^{1–3} or, for autonomous motors, by modifying the track sites that have been visited^{5,6,12}, by coupling motion to a unidirectional reaction cycle^{4,9,12} or by coordinating the conformation changes of different parts of the motor^{11,12}. DNA motors that satisfy all these criteria have typically been demonstrated on tracks that allow only 1–3 steps, although a stochastic DNA ‘spider’ with many legs has been shown to move longer distances by biased diffusion¹⁷ along a 100 nm track¹⁸.

We have investigated the motion of a simple directional and processive motor fuelled by DNA hydrolysis⁶ along an extended track consisting of a one-dimensional array of single-stranded attachment sites (stators), separated by ~6 nm. An extended track of 15 identical stators, flanked with special start and stop stators⁶, was assembled on a rectangular DNA origami tile measuring ~100 nm × 70 nm (ref. 16; Fig. 1, Supplementary Figs S1, S2). The tile comprises a 7,249-nucleotide (nt) single-stranded DNA template (genome of bacteriophage M13) hybridized to short synthetic staple strands such that the final tile consists of a raft of 24 parallel double helices tethered by the crossover of staples. Two tile designs were used. The helices of tile type A are crosslinked at 16 bp intervals, creating slight underwinding (10.7 bp per turn), which is expected to lead to a global right-handed twisting of the tile¹⁹. Tile type B is designed to reduce this twist: the average distance between crossovers is 15.6 bp (giving 10.4 bp per turn). The centre and ends of each staple are positioned on opposite surfaces of the tile. Selected staples were extended to include either the 22-nt stator sequence at the 5′ end or a hairpin at the centre¹⁶

(Fig. 1a). Stators hybridized to complementary motor strands are visible in atomic force microscope (AFM) images. Figure 1c shows the array of stators running diagonally across the tile with a separation of 6 nm, with the hairpin-modified staples forming two parallel lines that act as reference markers for image registration in some measurements.

The motor is a single strand of DNA that is complementary to a stator. A motor–stator duplex contains the recognition site for a nicking restriction enzyme that catalyses hydrolysis of a specific backbone linkage of the stator²⁰. The released energy drives movement of the motor from the cut stator to an adjacent intact stator⁶. The length of the cut stator–motor duplex (16 bp ≈ 5.44 nm) is similar to the spacing between stators (~6 nm). Figure 1b shows

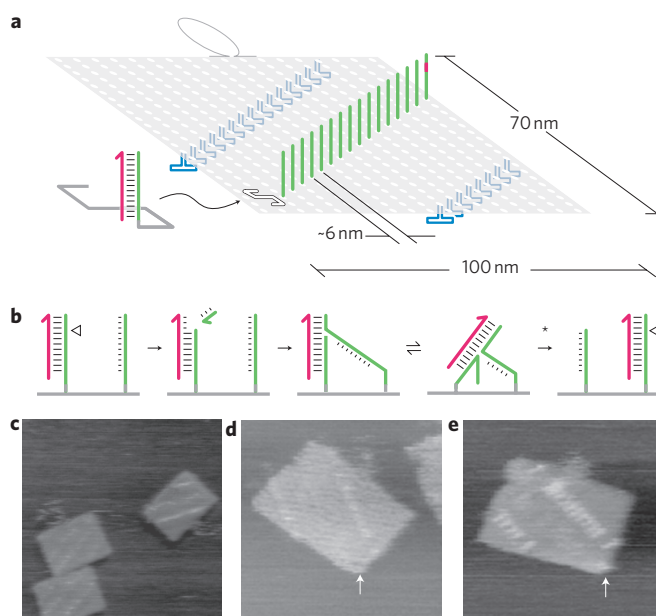


Figure 1 | DNA motor and track. a, Layout of the DNA origami tile, bearing the single-stranded stators of the track (green) and two rows of hairpin loops (blue) on opposite surfaces. **b**, Motor mechanism: a nicking enzyme cuts the motor-bound stator revealing a toehold at the 3′ end of the motor (magenta) that facilitates transfer of the motor to the adjacent intact stator by branch migration. **c**, AFM image of track with all stators decorated with motor. **d,e**, Motor can be precisely positioned on the track by omitting the first stator during tile assembly (**d**) then repairing the tile by addition of the missing stator hybridized to the motor (**e**).

¹University of Oxford, Department of Physics, Clarendon Laboratory, Parks Road, Oxford OX1 3PU, UK, ²Institute for Integrated Cell-Material Sciences (iCeMS), Kyoto University, Yoshida-ushinomiya-cho, Sakyo-ku, Kyoto 606-8501, Japan, ³Core Research for Evolutional Science and Technology (CREST), Japan Science and Technology Corporation (JST), Sanbancho, Chiyoda-ku, Tokyo 102-0075, Japan, ⁴Department of Chemistry, Graduate School of Science, Kyoto University, Kitashirakawa-oiwakecho, Sakyo-ku, Kyoto 606-8502, Japan. *e-mail: h.s@kuchem.kyoto-u.ac.jp; a.turberfield@physics.ox.ac.uk

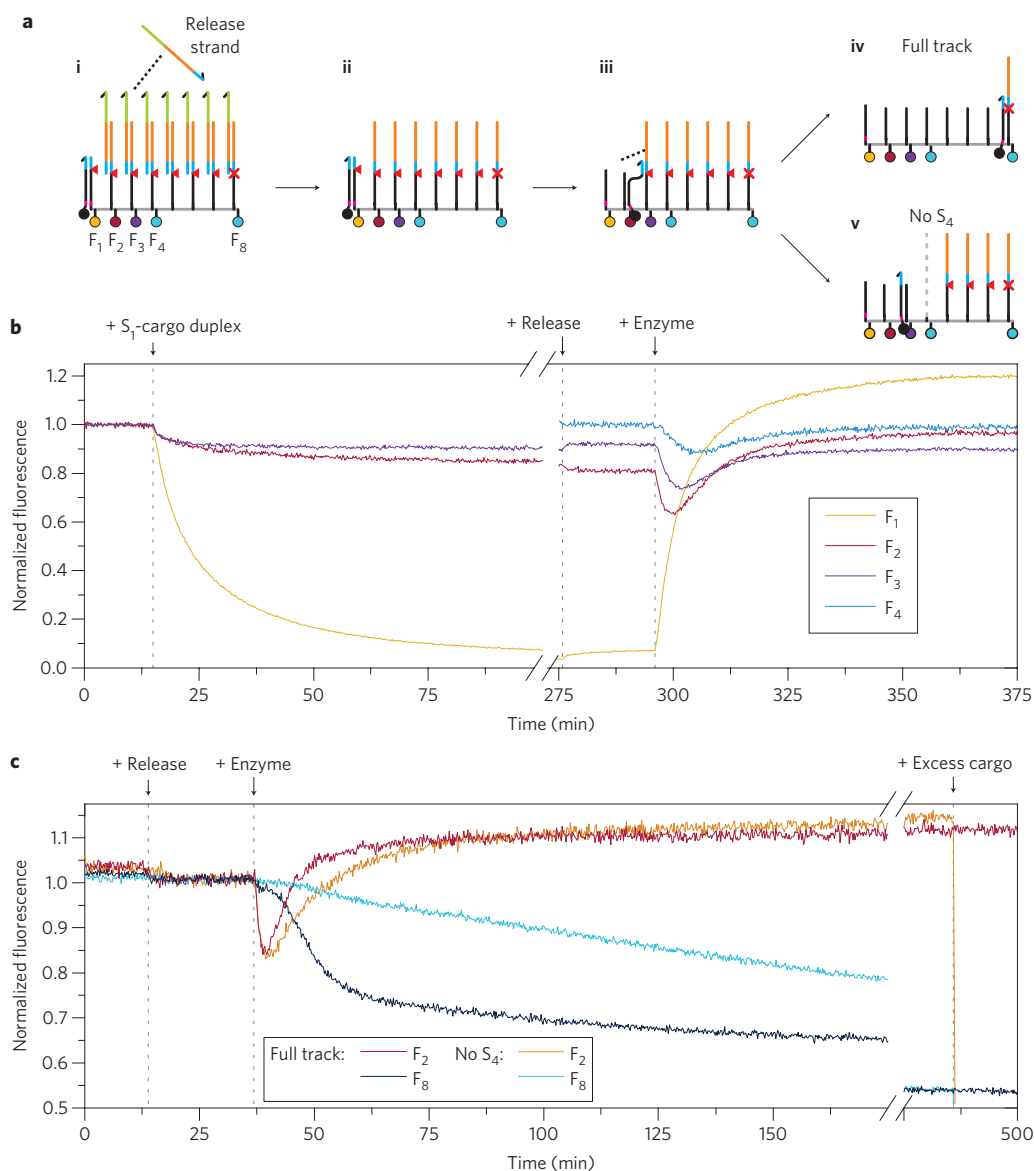


Figure 2 | Fluorescence measurements of movement on intact and broken tracks. **a**, Designed operating sequence. A motor carrying a quencher (Q) is loaded at position S_1 of an eight-stator track. Blocking strands occupy stators S_2 – S_8 , preventing movement of the motor. (i) Addition of release strand removes the blockade (ii). Active motion (iii) is triggered by addition of enzyme. Motor position is reported by quenching of fluorophores F_1 , F_2 , F_3 , F_4 and F_8 by the motor. **b**, Tracks labelled at F_1 and F_3 or F_1 and F_4 mixed with tracks labelled at F_2 . **c**, Fluorescence from tracks labelled at F_2 , F_8 . The quenching of F_8 that reports the arrival of motor at the end of an intact track is greatly reduced on tracks where stator S_4 is omitted.

the designed transfer mechanism: thermal dissociation of the 6-nt cut fragment is followed by strand exchange initiated by hybridization of the bases revealed at the 3' end of the motor. Directional movement is imposed because all stators in the wake of the motor have been cut (a 'burnt bridges' mechanism). The first stator forms two extra base pairs with the motor to help bias the initial motor position. The last stator has a modified sequence that creates a mismatch in the motor–stator duplex, protecting it from the enzyme and trapping the motor⁶.

To observe motor operation by ensemble fluorescence measurements, the motor was modified to carry a quenching group past a sequence of fluorophores at specific locations along the track. An eight-stator track (S_1 – S_8) on a type B tile was used for fluorescence experiments: the motor was loaded at S_1 and trapped at S_8 . The motor was loaded at a specific position by omitting the staple bearing the corresponding stator when the tile was assembled (Fig. 1d) then inserting the staple, bearing the motor, by incubating

it with the defective tile at room temperature (Fig. 1e; Supplementary Figs S3, S4). To prevent diffusion of the motor along the track before initiation of active transport, stators S_2 – S_8 were reversibly protected by addition of a blocking strand that hybridizes to a domain added at the 5' ends of these stators and the first 6 nt of the binding site of the motor. The blocking strand contains a 15-nt single-stranded toehold^{21,22} that allows the track to be activated by addition of a complementary release strand (Fig. 2a).

Figure 2b shows signal from fluorophores F_1 , F_2 , F_3 and F_4 positioned near stators S_1 , S_2 , S_3 and S_4 , respectively. To prevent Förster resonance energy transfer (FRET) between closely spaced fluorophores, tiles labelled with F_1 and F_3 or F_1 and F_4 , and tiles labelled with F_2 were prepared separately then mixed and observed at 37 °C. F_1 fluorescence decreases upon addition of a stoichiometric amount of the S_1 –motor duplex, consistent with loading of the motor at the first track position. Fluorescence at the other positions is largely

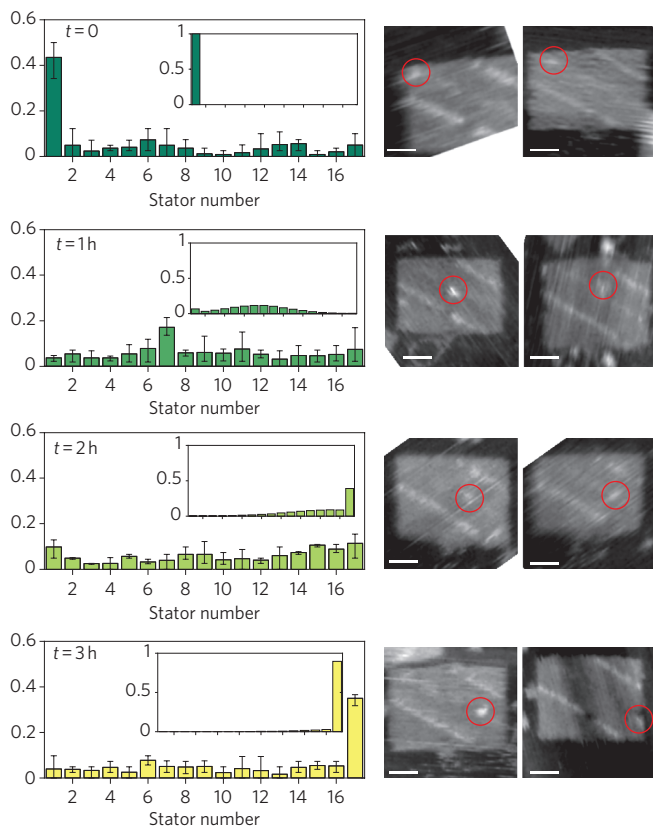


Figure 3 | Observation of motor movement by AFM. Seventeen-stator tracks with motor loaded at position S_1 were incubated with nicking enzyme at 23 °C. The distribution of motor positions before addition of enzyme and after 1, 2 and 3 h were determined by AFM. Representative images and histograms of motor positions are shown for each time point. Inset: motor distributions predicted by a simple kinetic model (Supplementary Fig. S5) using rate constants one-quarter of those deduced from fluorescence measurements on a short test track (the motor is slowed by the lower temperature and different buffer conditions required for AFM measurements, Supplementary Fig. S6). Scale bars, 20 nm.

unchanged, demonstrating that there is very little transfer of the motor to the blocked stators S_2 – S_8 . A slight increase in F_1 and slight decreases in F_2 – F_4 signals were observed when the release strand was added, consistent with slow diffusion of the motor.

When directed movement was initiated by addition of the nicking enzyme, an immediate increase in F_1 signal was observed, indicating motion of the motor away from S_1 as it is cut. Sequential, transient dips in F_2 , F_3 and F_4 signals indicate that the motor has occupied and then moved past stators S_2 , S_3 and S_4 in turn as they, too, are cut. After 30 min, the signals of all fluorophores return to a high steady state, consistent with accumulation of the motor strand at the distal end of the track. Figure 2c also shows the results of a similar experiment in which stators S_2 and S_8 were labelled. The same transient quenching of F_2 is observed, then the F_8 signal slowly and permanently decreases as the motor accumulates at the final stator. A simple model for stepping using first-order rate constants obtained from experiments on a short track⁶ agrees quantitatively with the data (Supplementary Fig. S5): the average motor speed is of the order of 0.1 nm s^{-1} .

When stator S_4 is omitted, leaving a 12 nm gap in the track, the rate of quenching of the F_8 signal falls (Fig. 2c), consistent with a strongly reduced stepping rate cross the gap. Increasing the size of the gap from 12 nm to 18 nm, and positioning the gap directly before the final mismatched stator, further decreases the rate at

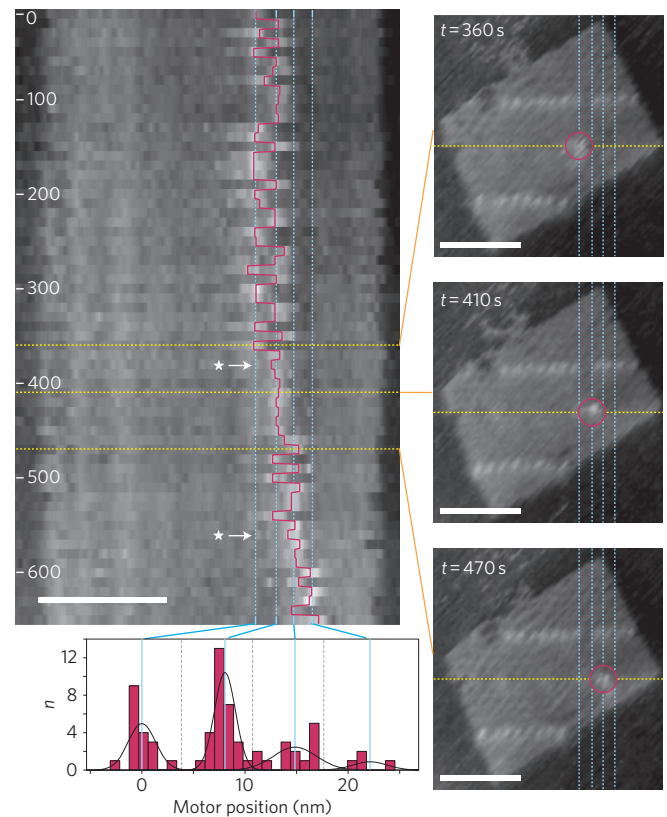


Figure 4 | AFM observation of discrete steps of a single motor molecule.

The main panel shows a kymograph, a stack of slices from successive frames, collected at 0.1 Hz, that correspond to the height profile along the track (3 of the 65 frames are shown on the right). The highest point on each profile, interpreted as the motor position, is marked; the histogram shows motor position relative to the first position observed. The motor steps between four stators (blue lines). Periods of rapid movement between adjacent stators are followed by slower transitions (*) in which the motor advances a single step. Scale bars, 50 nm. Timescale for the kymograph is in seconds.

which the motor reaches the end of the track (Supplementary Fig. S7). Changing the step size along the track by omitting stators can therefore be used to create a programmable delay.

Control experiments indicate that undriven stepping between stators is an order of magnitude slower than stepping driven by enzymatic cleavage (Supplementary Fig. S10). Transfer of motor strands between tiles in solution was measured both during normal stepping (Supplementary Fig. S9) and when the motor was delayed by a gap (Supplementary Fig. S8): inter-tile transfer occurs 5,000 times more slowly than stepping, and makes a negligible contribution to the transport of the motor to the end of the track.

A high-speed AFM imaging system^{23,24} was used to observe transport of individual motor molecules along full, 17-stator tracks on a type A tile. Tracks were prepared with the motor at S_1 as described above (but without the use of blocking strands), incubated with nicking enzyme for 0, 1 or 3 h at 23 °C, then deposited on mica and observed. The distribution of measured motor positions at each time point is shown in Fig. 3. Of the tiles with a detectable motor–stator duplex, 43% are located on S_1 at the initial time point, with the rest approximately uniformly distributed along the track. The distribution shifts progressively down the track: by 3 h, 35% of detectable motor has reached the end of the track. When stator S_7 is omitted, motor accumulates at S_6 (Supplementary Fig. S11), confirming our inference from fluorescence

measurements that the motor visits each stator in turn and is delayed when it encounters a break in the track.

The 0.1 s^{-1} AFM frame rate was sufficient to capture the stepping of individual motor strands in real time. Tiles loaded with motor, without control of its initial position, were incubated briefly with enzyme then washed to remove excess enzyme and observed in buffer. A kymograph representing the evolution of the measured height distribution along a track on which stepping was observed (Supplementary Movie S1) is shown in Fig. 4. Stepping occurs between four well-resolved, equally spaced positions on the track, which we interpret as consecutive stators. The step size is $7.4(\pm 1.0) \text{ nm}$, consistent with the spacing between stators. In most regions of the kymograph the motor moves back and forth between adjacent stators with a mean transition time that is similar to or shorter than the AFM frame time. We propose that this corresponds to incomplete migration of the motor between a cut stator and an adjacent intact stator. Two transitions (marked *) can be identified at which the motor progresses irreversibly by one stator. We interpret these transitions as complete transfer of the motor to the intact stator (marked * in Fig. 1b) at which it dwells, for 100 s and 50 s in the two occurrences observed, before starting to step to the downstream stator. We infer that cleavage of the stator occurs during the dwell time, catalysed by an enzyme that remains bound to the track. Similar transitions between two or three adjacent stators were observed on other tracks (Supplementary Figs S12, S13, Movie S2). Most motors were static, consistent with dissociation of enzyme from the tracks on washing. In all cases for which movement was observed, the tiles were oriented such that the tracks faced towards the mica surface, possibly reducing enzyme dissociation. Height profiles of the motor in these images are consistent with the presence of enzyme (Supplementary Fig. S15).

We have demonstrated the controlled operation of a synthetic molecular transporter over a 100 nm track. Motion is uniform, directional and processive. Experiments with broken tracks confirmed that the motor does not dissociate—it is only displaced from a cut stator by transfer to an intact stator, and is always bound to the track by hybridization of at least 16 nucleotides. Successful modelling of both fluorescence and AFM results supports our conclusion that the average time per step is constant, independent of distance travelled. The motor is programmably delayed by a gap in the track, and the step size could be used to tune the dwell time at each stator to the required coupling time for assembly steps. Using high-speed, real-time AFM we have observed discrete steps of a single motor. The two-dimensional DNA origami template could be used to create more complex track geometries, for example, junctions at which the motor could choose a path based on instructions encoded in the track or motor. The DNA tiles themselves can be concatenated^{16,25,26}, providing for cell-scale modular architectures that may be reprogrammed in solution. The uniform, long-range motion achieved is suitable for integration with a molecular assembly line²⁷ to create an autonomous molecular manufacturing system or synthetic ribosome. Precise control over both assembly and movement opens the way for the design of integrated systems that incorporate active transport and information processing.

Received 2 November 2010; accepted 22 December 2010;
published online 6 February 2011

References

- Shim, J.-S. & Pierce, N. A. A synthetic DNA walker for molecular transport. *J. Am. Chem. Soc.* **126**, 10834–10835 (2004).
- Sherman, W. B. & Seeman, N. C. A precisely controlled DNA biped walking device. *Nano Lett.* **4**, 1203–1207 (2004).

- Tian, Y. & Mao, C. A pair of DNA circles continuously rolls against each other. *J. Am. Chem. Soc.* **126**, 11410–11411 (2004).
- Yin, P., Yan, H., Daniell, X. G., Turberfield, A. J. & Reif, J. H. A unidirectional DNA walker that moves autonomously along a DNA track. *Angew. Chem. Int. Ed.* **43**, 4906–4911 (2004).
- Tian, Y., He, Y., Peng, Y. & Mao, C. A DNA enzyme that walks processively and autonomously along a one-dimensional track. *Angew. Chem. Int. Ed.* **44**, 4355–4358 (2005).
- Bath, J., Green, S. J. & Turberfield, A. J. A free-running DNA motor powered by a nicking enzyme. *Angew. Chem. Int. Ed.* **44**, 4358–4361 (2005).
- Pei, R. *et al.* Behaviour of polycatalytic assemblies in a substrate-displaying matrix. *J. Am. Chem. Soc.* **128**, 12693–12699 (2006).
- Venkataraman, S., Dirks, R. M., Rothmund, P. W. K., Winfree, E. & Pierce, N. A. An autonomous polymerization motor powered by DNA hybridization. *Nature Nanotech.* **2**, 490–494 (2007).
- Yin, P., Choi, H. M., Calvert, C. R. & Pierce, N. A. Programming biomolecular self-assembly pathways. *Nature* **451**, 318–322 (2008).
- Green, S. J., Bath, J. & Turberfield, A. J. Coordinated chemomechanical cycles: a mechanism for autonomous molecular motion. *Phys. Rev. Lett.* **101**, 238101 (2008).
- Bath, J., Green, S. J., Allen, K. E. & Turberfield, A. J. Mechanism for a directional, processive and reversible DNA motor. *Small* **5**, 1513–1516 (2009).
- Omabegho, T., Sha, R. & Seeman, N. C. A bipedal Brownian motor with coordinated legs. *Science* **324**, 67–71 (2009).
- Turberfield, A. J. *et al.* DNA fuel for free-running nanomachines. *Phys. Rev. Lett.* **90**, 118102 (2003).
- Bois, J. S. *et al.* Topological constraints in nucleic acid hybridization kinetics. *Nucleic Acids Res.* **33**, 4090–4095 (2005).
- Green, S. J., Lubrich, D. & Turberfield, A. J. DNA hairpins: fuel for autonomous DNA devices. *Biophys. J.* **91**, 2966–2975 (2006).
- Rothmund, P. W. K. Folding DNA to create nanoscale shapes and patterns. *Nature* **440**, 297–302 (2006).
- Antal, T. & Krapivsky, P. L. Molecular spiders with memory. *Phys. Rev. E* **76**, 021121 (2007).
- Lund, K. *et al.* Molecular robots guided by prescriptive landscapes. *Nature* **465**, 206–210 (2010).
- Dietz, H., Douglas, S. M. & Shih, W. M. Folding DNA into twisted and curved nanoscale shapes. *Science* **325**, 725–730 (2009).
- Heiter, D., Lunnen, K. D. & Wilson, G. G. Site-specific DNA-nicking mutants of the heterodimeric restriction endonuclease R.BbvCI. *J. Mol. Biol.* **348**, 631–640 (2005).
- Yurke, B., Turberfield, A. J., Mills, A. P. Jr, Simmel, F. C. & Neumann, J. L. A DNA-fuelled molecular machine made of DNA. *Nature* **406**, 605–608 (2000).
- Yurke, B. & Mills, A. P. Jr. Using DNA to power nanostructures. *Genet. Program. Evol. Mach.* **4**, 111–122 (2003).
- Ando, T. *et al.* High-speed atomic force microscope for studying biological macromolecules. *Proc. Natl Acad. Sci. USA* **98**, 12468–12472 (2001).
- Endo, M., Katsuda, Y., Hidaka, K. & Sugiyama, H. Regulation of DNA methylation using different tensions in the double strands constructed in a defined DNA nanostructure. *J. Am. Chem. Soc.* **132**, 1592–1597 (2010).
- Endo, M., Sugita, T., Katsuda, Y., Hidaka, K. & Sugiyama, H. Programmed-assembly system using DNA jigsaw pieces. *Chem. Eur. J.* **16**, 5362–5368 (2010).
- Douglas, S. M. *et al.* Self-assembly of DNA into nanoscale three-dimensional shapes. *Nature* **459**, 414–418 (2009).
- Gu, H., Chao, J., Xiao, S. J. & Seeman, N. C. A proximity-based programmable DNA nanoscale assembly line. *Nature* **465**, 202–205 (2010).

Acknowledgements

This work was supported by the Engineering and Physical Sciences Research Council (EP/G037930/1), the Clarendon Fund, the Oxford–Australia Scholarship Fund, the CREST of JST and a Grant-in-Aid for Science Research from the Ministry of Education, Culture, Sports, Science and Technology, Japan.

Author contributions

Experiments were designed by S.W. with input from J.B. and A.J.T. Ensemble fluorescence experiments were carried out by S.W. in the laboratory of A.J.T. Real-time AFM experiments were done by S.W., M.E., Y.K. and K.H. in the laboratory of H.S. The manuscript was written by S.W., J.B., H.S. and A.J.T.

Additional information

The authors declare no competing financial interests. Supplementary information accompanies this paper at www.nature.com/naturenanotechnology. Reprints and permission information is available online at <http://npg.nature.com/reprintsandpermissions/>. Correspondence and requests for materials should be addressed to H.S. and A.J.T.